

Article

Supercritical CO₂ Assisted Electro spray to Produce Poly(lactic-co-glycolic Acid) Nanoparticles

Elena Barbero-Colmenar¹, Mariangela Guastaferro², Lucia Baldino^{2,*} , Stefano Cardea² 
and Ernesto Reverchon² 

¹ Department of Chemical Engineering, Universitat Rovira i Virgili, E-43007 Tarragona, Spain

² Department of Industrial Engineering, University of Salerno, Via Giovanni Paolo II, 132, 84084 Fisciano, Italy

* Correspondence: lbaldino@unisa.it

Abstract: This work proposes an improvement of the traditional electro spraying process, in which supercritical carbon dioxide (SC-CO₂) is used to produce poly(lactic-co-glycolic acid) (PLGA) nanoparticles. The experiments were performed at different PLGA concentrations (1, 3 and 5% *w/w*), applied voltages (10 and 30 kV) and operating pressures (80, 120 and 140 bar). It was found that working at 140 bar and 30 kV, spherical nanoparticles, with mean diameters of 101 ± 13 nm and 151 ± 45 nm, were obtained, when solutions at 1% *w/w* and 3% *w/w* PLGA were electro sprayed, respectively. Increasing PLGA concentration up to 5% *w/w*, a mixture of fibers and particles was observed, indicating the transition to the electro spinning regime.

Keywords: electro spray; electrohydrodynamic atomization; supercritical CO₂; nanoparticles; biopolymer; poly(lactic-co-glycolic acid)



Citation: Barbero-Colmenar, E.; Guastaferro, M.; Baldino, L.; Cardea, S.; Reverchon, E. Supercritical CO₂ Assisted Electro spray to Produce Poly(lactic-co-glycolic Acid) Nanoparticles. *ChemEngineering* **2022**, *6*, 66. <https://doi.org/10.3390/chemengineering6050066>

Academic Editors: Alirio E. Rodrigues and Andrew S. Paluch

Received: 21 July 2022

Accepted: 24 August 2022

Published: 1 September 2022

Publisher's Note: MDPI stays neutral with regard to jurisdictional claims in published maps and institutional affiliations.



Copyright: © 2022 by the authors. Licensee MDPI, Basel, Switzerland. This article is an open access article distributed under the terms and conditions of the Creative Commons Attribution (CC BY) license (<https://creativecommons.org/licenses/by/4.0/>).

1. Introduction

The use of biodegradable polymers loaded with active compounds plays an important role in the production of micro and nanoparticles for different applications, such as biomedical, nutraceutical and pharmaceutical [1,2]. Composite micro and nanoparticles are especially attractive for drug delivery and therapeutic uses for several reasons: (i) their small size enhances drug bioavailability, (ii) the biopolymeric matrix increases the drug stability, (iii) a prolonged effect of the drug is possible as a result of a controlled release, and (iv) using a biodegradable and biocompatible polymer, there is no risk of intoxication or undesirable side effects [3,4].

Solvent evaporation methods (i.e., emulsion solvent, spray freeze drying, coacervation and liquid antisolvent precipitation) are commonly used for nanoparticle manufacturing [5–7], with spray drying being the most extended technique adopted in the pharmaceutical and food industries [8–10]. However, these methods show some drawbacks, such as a wide particle size distribution [11,12], low encapsulation efficiency [13–15] and complex particle recovery processes that lead to low production efficiency [4,16]. In addition to these problems, other limits are the use of toxic organic solvents that can remain in the final product, and the use of high temperatures that may damage the active principles encapsulated inside the biopolymeric nanoparticles [17].

Electro spray, also known as electrohydrodynamic atomization (EHDA), is a robust technique for producing particles with a controlled morphology [18] and size [19,20]. In this technique, a liquid pumped through a nozzle is electrically charged by applying a high voltage. The electrified liquid assumes a conical shape (the so-called Taylor cone) with a thin jet at its end. The jet, then, breaks up into highly charged droplets that form a charged spray plume and they drift towards an oppositely charged substrate, where they are collected as solid particles after the solvent evaporation [21]. Electro spray gained the interest of many researchers, due to its unique feature in producing quasi-monodisperse

particles over a wide range of sizes, from tens of nanometers to a few microns, without agglomeration phenomena [18,22]. Additional advantages of electrospraying, over the other liquid atomization techniques, are the high drug encapsulation efficiency, its versatility (different materials can be processed) and the inexpensive setup [23]. However, the following limits need to be overcome to extend this technique to industrial applications: (i) the low throughputs obtained with a single emitter (due to the low flow rates used for operating in a stable spraying mode), (ii) traces of solvents may remain entrapped in the particles after being collected, (iii) limited operation window for highly concentrated polymer solutions, mainly related to their viscosity [24].

Poly(lactic-co-glycolic acid) (PLGA) is a synthetic, biodegradable, biocompatible and non-toxic polymer, approved by US Food and Drug Administration (FDA) and European Medicine Agency (EMA) for its application in drug delivery [25]. In particular, PLGA is a versatile polymer, since it can be used in combination with either hydrophilic or hydrophobic drugs, and small or large molecules [25–27]. For these reasons, PLGA is one of the most promising and widely used biopolymers for drug delivery applications [3,4,28–34].

Numerous studies were carried out with the aim of producing PLGA microparticles with controlled and suitable morphologies for drug encapsulation, using electrospray. For example, Tanaka, et al. [33] studied the formation mechanisms of PLGA particles from the electrospray droplets. Different PLGA solutions were electrosprayed varying polymer concentration, molecular weight, applied voltage and working distance. As a result, agglomerated particles with sizes ranging from 0.6 to 6.6 μm and an irregular and porous morphology were obtained. Rezvanpour & Wang [31] aimed at increasing the collection efficiency of PLGA particles and used an additional electrode between the needle and the collector. They obtained particles between 3–6 μm and 6–12 μm , respectively. The auxiliary electric field enhanced the particle collection efficiency. Liu, et al. [30] proposed the electrospraying of PLGA-acetone solutions in different conditions, including high-pressure carbon dioxide and carbon dioxide-expanded hexane, to evaporate the solvent and to control the particle morphology. In particular, using carbon dioxide at 6.21 MPa in the spray chamber, they obtained a PLGA membrane, as a consequence of the polymer plasticization due to carbon dioxide. Ropivacaine and dexamethasone loaded PLGA microparticles were produced by Shen, et al. [32], using dimethylformamide (DMF) as a solvent. Microparticles with an average size ranging from $5.3 \pm 0.2 \mu\text{m}$ up to $6.6 \pm 0.2 \mu\text{m}$ were obtained when the polymer-to-drug ratios were 4:1 and 3:1, respectively. Nath, et al. [4] prepared simvastatin-PLGA loaded particles, obtaining particles with a mean diameter ranging from 2 to 8 μm , with a high polydispersity. Jahangiri, et al. [28] encapsulated triamcinolone acetonide into PLGA nanofibers and beads (drug to polymer ratios 1/5 and 1/10). Using acetone as a solvent, particles and fibers, sized between 50 and 1500 nm, with an irregular morphology, were obtained. Xu, et al. [34] produced doxorubicin loaded PLGA microparticles with different morphologies using various solvents; but only when tetrahydrofuran (THF) or DMF were used, spherical microparticles, between 1–3 μm , were obtained.

However, the previous works show scarce success in obtaining unimodal particles with a well-controlled morphology in the nanometric range. Moreover, the most challenging limitation to overcome is still the low throughput of this process, due to the low liquid flow rates processed in the traditional electrospraying.

A modification of the traditional electrospray process using supercritical fluids technology has been recently proposed to produce polyvinylpyrrolidone (PVP) microparticles [35,36]. The key aspect of this new method relies on the addition of supercritical carbon dioxide (SC-CO₂) to the polymer solution, which is electrified and discharged at room conditions as a gas expanded liquid (GXL) [37]. The solubilized CO₂ molecules interposed among the solvent molecules in the liquid phase, causing a considerable reduction in their interactions. This leads to a reduction of the solution viscosity and surface tension, which are the critical parameters in the transition between the droplet formation (electrospray) and the formation of a continuous liquid phase (electrospinning). Both properties are cohesive forces, being opposite to the liquid jet breakup and droplet formation. Therefore,

because of the addition of SC-CO₂, the atomization process would be favored. Operating in this way, liquid flow rates up to hundred times larger than in traditional electrospray can be processed [35,36,38,39]. Moreover, these authors established that the operating pressure was the key parameter determining the particle size and particle size distribution (PSDs), resulting in smaller particles with narrower PSDs when operating at higher pressures [35,36]. The increase of the applied voltage would promote the regularity of the atomization, leading to more homogeneous droplets and, as a result, sharper PSDs [36]. Increasing the polymer concentration and molecular weight, the solution viscosity increased; therefore, larger particles were obtained until the jet breakup did not happen anymore and microfibers were produced [36].

In conclusion, SC-CO₂ assisted electrospray is a suitable technology to produce polymeric micro and nanoparticles. However, to the best of our knowledge, PLGA nanoparticles with controlled size and spherical morphology have not been reliably produced by SC-CO₂ assisted electrospraying. Therefore, the scope of this work is to apply this technology with the aim of finding the optimal process conditions leading to the desired PLGA particle size (i.e., in the nanometric range) and morphology (i.e., spherical) for subsequent drug encapsulation. The effect of pressure, PLGA concentration and applied voltage on particles morphology were investigated in this study and a liquid collector was used for particles deposit.

2. Materials and Methods

2.1. Materials

Poly(lactic-co-glycolic acid) (RESOMER 504H, ratio 50:50, Mw 38,000–54,000 Da, indicated as high Mw-PLGA) was purchased from Evonik Industries (Essen, Germany); acetone (purity > 99.5%) and ethanol (purity > 99.9%) were purchased from Sigma Aldrich (Milan, Italy). CO₂ (99.9% purity) was supplied by Morlando Group Srl (Sant'Antimo (NA), Italy). All the chemicals were used without further purification.

2.2. Experimental Setup Description and Electrospraying Protocol

PLGA powder was dissolved in acetone at different concentrations by weight (1%, 3% and 5%), at room temperature and using a magnetic stirrer until its complete dissolution.

The setup used, shown in Figures 1 and 2, consisted of a stainless-steel high-pressure vessel (about 70 mL of internal volume), in which the PLGA-acetone solution was loaded. Using a high-pressure pump (Gilson, mod. 305, Middleton, WI, USA), CO₂ was pumped into the vessel from the bottom, up to the operating pressure. After 10 min of the system equilibration, during which the mixture between SC-CO₂ and PLGA solution was promoted to form a GXL, nitrogen was supplied from the top of the vessel at the same pressure selected for the process. After the opening of an ON/OFF valve (Swagelok ON/OFF, Nordival Srl, Rovato (BS), Italy), PLGA solution exited the vessel and was ejected through a narrow injector (140 µm internal diameter). The desirable electrical field was generated using a high-voltage power supply (HVPS) (FUG Elektronik, HCP 35-3500, Schechen, Germany). The environment of the injection system was warmed up using two infrared lamps (Efbe-Schott, 150 W, Germany) to promote solvent evaporation during the droplets flight to the collector, which consisted of an aluminum container filled with ethanol, placed 30 cm away from the injector. The temperature in the vessel was set at 35 or 40 °C, and it was measured using a type J thermocouple and adjusted using a PID controller (mod. 305, Watlow, Corsico (MI), Italy).

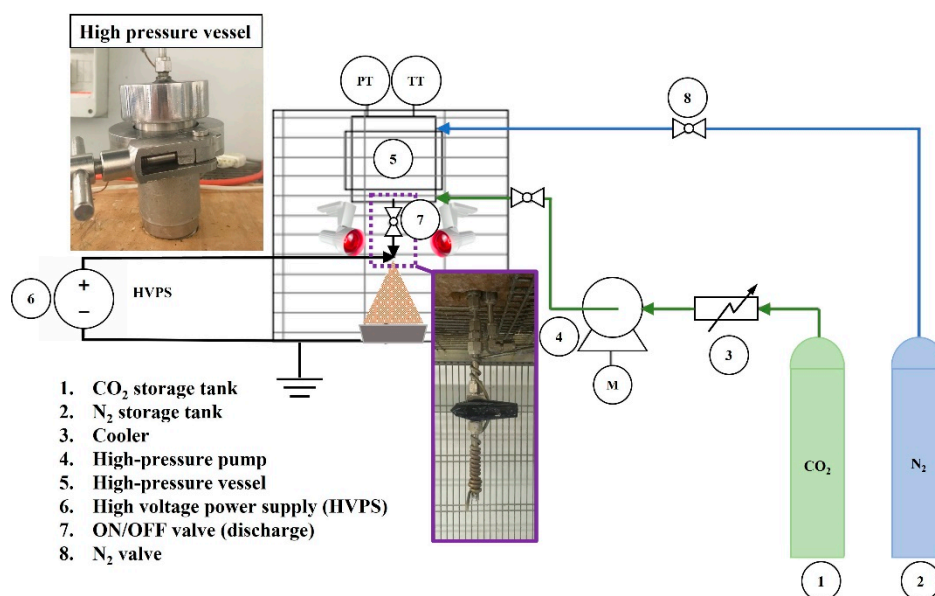


Figure 1. Representation of the setup used for PLGA nanoparticles production by supercritical CO₂ assisted electro spray.

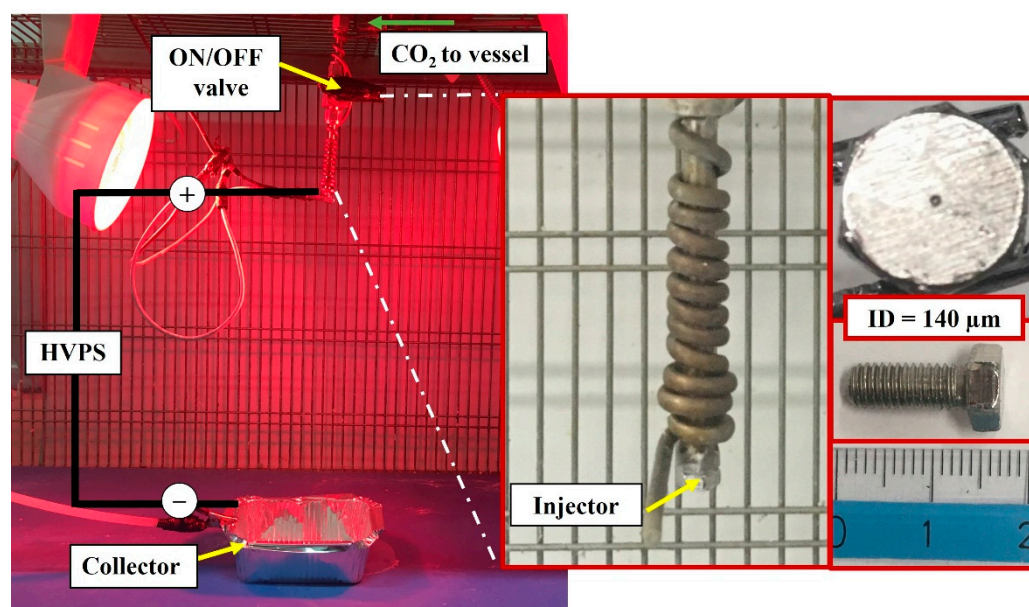


Figure 2. Real images of the spraying zone formed by the injector system elements and the collector used for nanoparticles deposit. The inset images show the detail of the injector used for these experiments.

2.3. Morphology and Particle Size Distribution

The mean diameter of the nanoparticles was measured by dynamic light scattering (DLS), using a Malvern Zetasizer instrument (Zetasizer Nano S, Malvern, UK). For this analysis, a 2 mL volume of the collected suspension was used without any further dilution steps. PSDs were computed using Microcal Origin Software (release 8.0, Microcal Software, Inc., Northampton, MA, USA).

Particles morphology was observed by a field emission scanning electron microscope with a focused ion beam, FESEM-FIB (FEI company Scios 2). Before being imaged, the samples were prepared as follows: samples from solutions at 1% w/w and 3% w/w PLGA were prepared by placing a few droplets of the nanoparticle suspension on a silicon wafer

piece, and the solvent was evaporated at room conditions before sample gold-coating. For the samples at 5% *w/w* PLGA, the solid residue formed after the test was analyzed directly after drying at room conditions. It was stuck on the carbon tape and gold-coated. In all cases, the gold-coating of the samples was performed using a sputter coater (Agar Auto Sputter Coater mod. 108 A, Stansted, UK) at 40 mA for 120 s.

3. Results and Discussion

3.1. Effect of Pressure and PLGA Concentration

This part of the study investigated the effect of the operating pressure on particle size and PSDs, using PLGA as a model biopolymer. Fixed PLGA concentrations at 1%, 3% and 5% *w/w*, operating pressures of 80, 120 and 140 bar were tested. The applied voltage and the collection distance were set at 30 kV and 30 cm, respectively, based on previous studies [36,38]. Using these pressure values, CO₂ is above the critical point when operating at 35–40 °C. PLGA concentrations were selected to operate within the electro spraying zone (particles production), according to the previous electro spraying/electro spinning literature [40].

Figure 3 reports PSDs of 1% *w/w* and 3% *w/w* PLGA particles, obtained by DLS. Particle mean diameters, standard deviations (SD) and polydispersity index (PDI) are also reported in Table 1. The results showed that processing a solution at 1% *w/w* PLGA, nanoparticles were produced at 80, 120 and 140 bar. The particle size decreased from 147 ± 52 nm to 133 ± 41 nm, when the operating pressure was increased from 80 to 120 bar, respectively. Particles with a mean size of 101 ± 13 nm were, instead, obtained at 140 bar. PDI results revealed that the most homogeneous particles were produced at higher values of operating pressure. Therefore, at this composition, the increasing of the operating pressure resulted in a reduction of the particles' mean diameter and sharper PSDs (Figure 3a). A most remarkable effect of the pressure on the particle size and PSDs was found operating at 3% *w/w* PLGA where nanoparticles were obtained at 80, 120 and 140 bar, with mean sizes of 230 ± 152 nm, 163 ± 76 nm and 151 ± 45 nm, respectively (Table 1). Again, it was demonstrated that operating at higher values of pressure led to the formation of smaller and monodisperse particles, with narrower PSDs (Figure 3b).

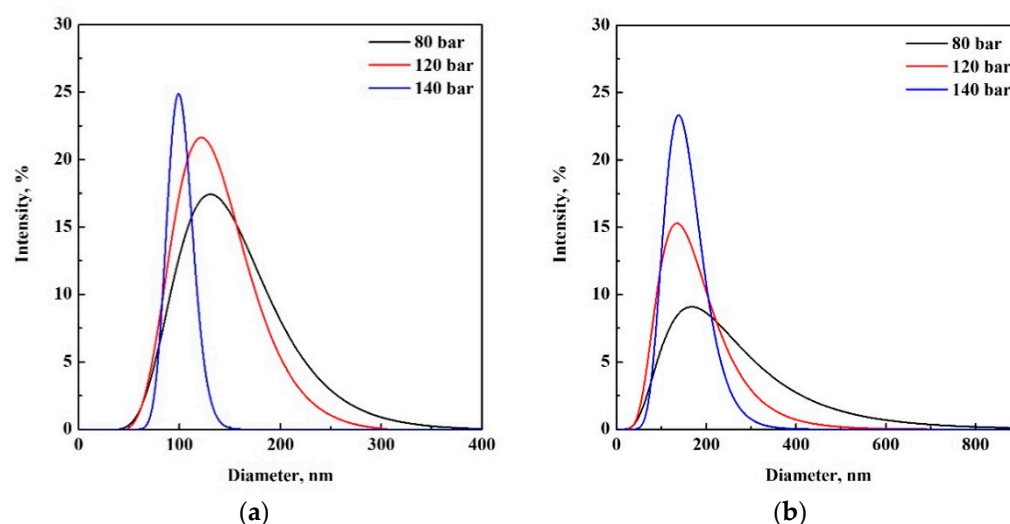


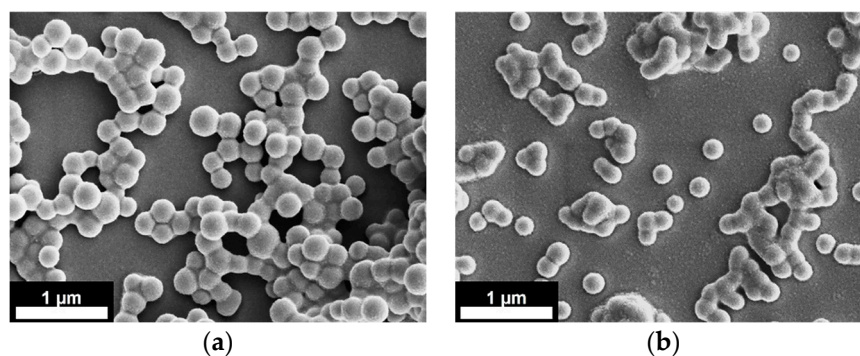
Figure 3. PSDs of samples produced by SC-CO₂ assisted electro spray at P = 80 bar (black), P = 120 bar (red) and P = 140 bar (blue); V = 30 kV and PLGA concentrations: (a) 1% *w/w* and (b) 3% *w/w*.

Table 1. Particles mean diameter, SD and PDI obtained at different PLGA concentrations and pressures; applied voltage 30 kV.

PLGA, % <i>w/w</i>	Pressure (bar)	Mean Diameter \pm SD, nm	PDI	Morphology
1	80	147 \pm 52	0.126	P
1	120	133 \pm 41	0.094	P
1	140	101 \pm 13	0.015	P
3	80	230 \pm 151	0.432	P
3	120	163 \pm 76	0.215	P
3	140	151 \pm 45	0.091	P
5	80	T	T	P/F
5	120	T	T	P/F
5	140	T	T	P/F

P = particles; F = fibers; T = transition zone.

SEM images of the PLGA nanoparticles, produced at 120 bar and 140 bar, are reported in Figure 4a,b for 1% *w/w* and 3% *w/w* PLGA, respectively.

**Figure 4.** SEM images of nanoparticles obtained from: (a) 1% *w/w* PLGA solution at 120 bar and (b) 3% *w/w* PLGA solution at 140 bar. Applied voltage 30 kV. Scale bars 1 μ m.

As it is shown in Figure 4 (and Table 1), when increasing polymer concentration (from 1% *w/w* to 3% *w/w*) and, at the same time, the operating pressure (from 120 bar to 140 bar), the PLGA nanoparticles were similarly sized. This behavior was due to the compensatory effect of the polymer concentration (the higher the polymer concentration the larger the particle size) and the operating pressure (the higher the operating pressure the smaller the particle size). A further explanation of these results could be provided by a dimensionless analysis, considering the Weber number, when additional effects related to viscosity and applied voltage are neglected [21]. The Weber number represents the ratio between the disruptive hydrodynamic forces and the stabilizing surface tension force. It is defined as $(\rho v^2 L / \sigma)$, where ρ is the fluid density, v is the velocity, L is the droplet diameter and σ is the surface tension of the fluid. Higher values of pressure could lead to larger Weber numbers, since the velocity of the liquid exiting the injector could be increased. In addition to this, when operating at higher pressure, a larger amount of CO_2 could be dissolved in the polymeric solution, forming a gas expanded liquid with lower surface tension [35]. Therefore, at higher pressure, the disruptive force exerted on the liquid jet is larger, promoting atomization and the production of smaller and more homogeneous particles.

Increasing PLGA concentration up to 5% *w/w*, a mixture of nanoparticles, microparticles and fibers was found in all the collected samples. Figure 5 shows the morphology of the obtained hybrid structures when the process was operated at 140 bar, which is a representative image of the results obtained at 5% *w/w* PLGA. These findings proved that, at this PLGA concentration, the transition zone between electrospray (particles) and electrospinning (fibers) occurred. PSDs corresponding to this polymer concentration are

not reported in Figure 3, because the measurements of particle sizes performed using DLS would not be representative, since a significant part of the polymer was formed by fibers.

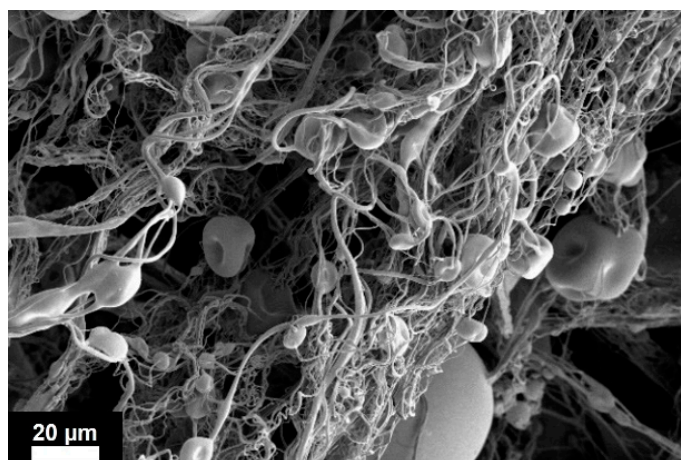


Figure 5. SEM image of 5% *w/w* PLGA fibers/particles obtained from the solid residue produced at 140 bar. Applied voltage 30 kV. Scale bar 20 μm.

The results obtained using PLGA agreed with the previous studies reported in the literature related to PVP [35,36] and cellulose acetate [39] processed by SC-CO₂ assisted electrospay. In those cases, a dependence of the particle diameter on the operating pressure was demonstrated, resulting in smaller and more monodisperse particles when operating at higher pressure values [35,36,38,39]. Previous results reported by Baldino, et al. [36] demonstrated that the transition from supercritical electrospaying to electrospinning could be shifted to higher polymer concentrations by increasing the operating pressure. These authors found that when PVP 1300 kDa was used and operating at 100 bar, the transition from microparticles to microfibers occurred at 7% *w/w* PVP; whereas, operating at 120 bar, the transition between the two morphologies moved to 10% *w/w* PVP.

In the case of PLGA, the increase of the operating pressure did not avoid the fiber formation since, processing 5% *w/w* PLGA solution, fibers were formed even at 140 bar. The transition between both regimes depended strongly on the polymer concentration; but also on other intrinsic polymer properties, such as molecular weight and viscosity.

Regarding the effect of polymer concentration on particles' morphologies, the results showed that, increasing the amount of polymer, particles average diameter increased (Table 1), because of the larger solution viscosity which led to the formation of larger droplets. An important effect of the polymer concentration is the transition from particulate to fibrous morphology that was found at about 5% *w/w* PLGA. This is in agreement with the results reported in the literature by Husain, et al. [40], when PLGA of the same range of molecular weight (i.e., 33 kDa) was used. These authors used traditional electrospay to process solutions of PLGA in acetone at different concentrations and found that, operating at 15 kV and at a fixed liquid flow rate of 50 μL/min, the electrospaying regime (only particles production) occurred between 2% *w/w* and 4% *w/w*; whereas, a mixture of particles and beads-on-strings was obtained at concentrations between 10% *w/w* and 15% *w/w*. Above these polymer concentration values, only fibers were obtained.

It is important to mention that, for the tested conditions, we did not observe any signal of particles lost (there was no particle deposition on electrodes or solid residue inside the vessel). In addition, it was qualitatively observed how the entire droplets of spray reached the liquid collector, where they were collected as solid nanoparticles. This is not surprising, because the charged droplets are expected to follow predictable trajectories, ruled by the electrical field lines. For these reasons, it is expected a process yield, in terms of mass, close to 100%. This high yield of the SC-CO₂ assisted process is coherent with the yield reported in previous electrospay works in the literature. Carrasco, et al. [41] prepared

polystyrene (PS) microparticles using traditional electrospray. The authors reported a collection efficiency of the polymeric particles into a membrane filter near 100%.

3.2. Effect of the Applied Voltage

In the traditional electrospray process, the applied voltage is, together with the liquid flow rate, the most relevant parameter for achieving a stable cone-jet mode and obtaining highly monodispersed particles. Indeed, applying a high voltage, the polymeric liquid is largely electrified, overcoming surface tension and forming a stable conical meniscus (Taylor cone) where a very tiny liquid jet emerges and breaks up into very small, charged droplets [42]. The shape of this liquid cone is a result of the balance of several forces: liquid surface tension, liquid pressure, gravity, electric stresses in the liquid surface, liquid inertia, and liquid viscosity [42,43]. When operating in stable cone-jet mode, size is not significantly affected by voltage and only a slight decrease in size is observed when voltage is increased [17]. However, the particle size distribution depends on the diameter of the jet and on the breakup pattern, which is determined by the balance of the above-mentioned involved forces.

Therefore, to investigate whether the applied voltage had an effect on particle size and PSDs in the case of SC-CO₂ assisted electrospray, the experiments were carried out using the solution at 3% *w/w* PLGA, setting the voltage at 10 kV and operating at 80 and 140 bar. PSDs of these samples are shown in Figure 6; whereas Table 2 reports mean size, SD and PDI of the produced PLGA particles.

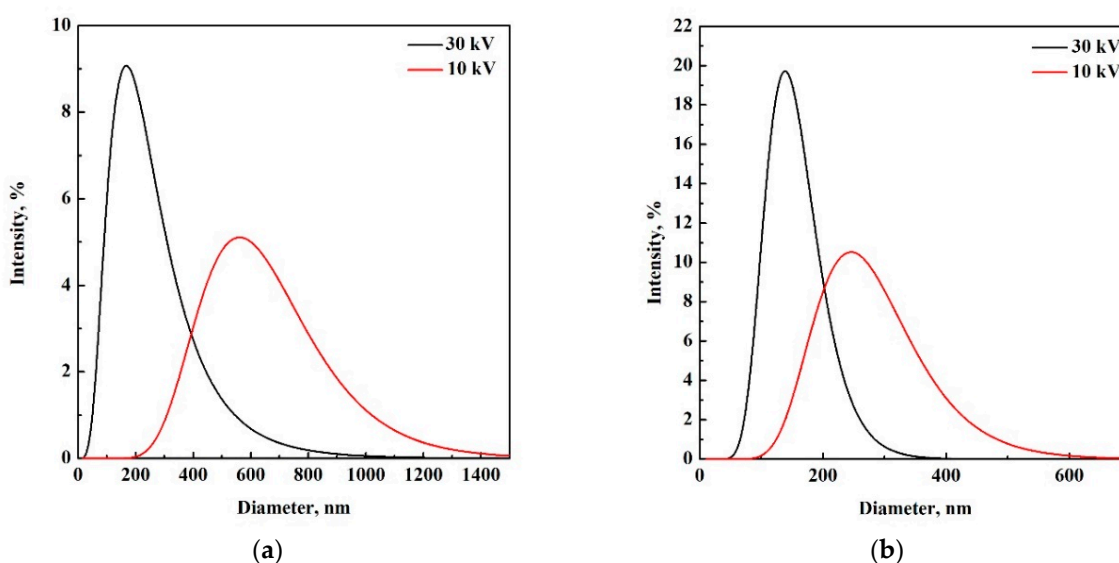


Figure 6. PSDs of samples produced by SC-CO₂ assisted electrospray at 3% *w/w* PLGA and 10 kV (red) and 30 kV (black), when operating at: (a) 80 bar and (b) 140 bar.

Table 2. Particles mean diameter, SD and PDI of samples produced at 3% *w/w* PLGA, varying the applied voltage (10 and 30 kV) and the operating pressure (80 and 140 bar). Morphology: particles.

Pressure (bar)	Voltage (kV)	Mean Diameter \pm SD (nm)	PDI
80	10	626.4 \pm 213.3	0.116
80	30	230.0 \pm 151.5	0.434
140	10	270.6 \pm 86.6	0.102
140	30	150.8 \pm 45.5	0.091

Operating at 10 kV, nanoparticles were produced for both values of pressure. When operating at 80 bar, the decrease of applied voltage from 30 to 10 kV led to an increment of particle mean size, from 230 to 626 nm, respectively. PSDs became broader as well,

increasing standard deviation from 152 to 213 nm. Operating at 140 bar, the same trend was observed; particle mean size increased from 151 to 270 nm, and standard deviation increased from 46 to 87 nm, when the voltage was reduced from 30 kV to 10 kV, respectively. These results demonstrated that, at higher voltage, particles with a smaller mean diameter and sharper particle size distribution were formed, as summarized in Table 2 and Figure 6a,b. This effect was more remarkable when operating at a lower pressure (i.e., 80 bar) and it could be explained by considering that applied voltage and pressure were acting as disruptive forces against viscosity and surface tension (cohesive forces), favouring the liquid atomization. Therefore, operating at higher voltage and pressure, the atomization process was favored, promoting the formation of more regular and smaller droplets and, as a consequence, monodisperse particles with smaller sizes could be obtained. As it is shown in Table 2, in this study, the smallest and most monodisperse particles (i.e., with smaller PDI) were obtained at 30 kV and 140 bar.

4. Conclusions

Biocompatible and spherical nanoparticles formed by PLGA were successfully produced using SC-CO₂ assisted electrospray. The addition of SC-CO₂ to the precursor polymeric solution was crucial, since it would promote the formation of a GXL, reducing the surface tension and viscosity of the solution and, as a result, improving the atomization process.

For a polymer concentration of 1% *w/w* and 3% *w/w*, the increment of the operating pressure, from 80 bar to 140 bar, resulted in a reduction of the particle mean size coming along with a narrowing of the particle size distribution. The increase in PLGA concentration up to 5% *w/w*, promoted the formation of fibers and highlighted the transition from electrospraying to electrospinning. The effect of the applied voltage was also investigated for the solution at 3% *w/w* PLGA, and it was found that, when operating at 140 bar, smaller particles with narrower PSDs were produced when the applied voltage was higher. Among all the conditions tested, the smallest and more monodispersed particles were obtained processing 1% *w/w* PLGA solution, at 30 kV and 140 bar.

Like other spray-based methods, such as electrospray, SC-CO₂ assisted electrospray enables the production of small and monodisperse particles with a high yield. Moreover, unlike traditional electrospray, using the proposed methodology, the liquid flow of the processed solution can be increased up to three orders of magnitude, resulting in higher throughputs that preserve, at the same time, uniform and regular particle morphology. Summarizing, these results confirm the feasibility and versatility of SC-CO₂ assisted electrospray technology for the production of nano and microparticles, as well as microfibers, with suitable morphology and size to be used as drug carriers for biomedical and pharmaceutical applications.

Author Contributions: Conceptualization, L.B. and E.R.; Methodology, L.B., S.C. and E.R.; Investigation, E.B.-C. and M.G.; Formal analysis, E.B.-C., M.G. and L.B.; writing—original draft, E.B.-C.; writing—review and editing, M.G., L.B., S.C. and E.R.; supervision, L.B. and E.R.; funding acquisition, E.R. All authors have read and agreed to the published version of the manuscript.

Funding: This research received no external funding.

Data Availability Statement: Not applicable.

Acknowledgments: E.B.-C. acknowledges the Spanish Government scholarship BES-2016-077914 (MINECO/AEI/FEDER, UE) and the founding obtained from the grant PGC2018-099687-B-I00 (MCI/AEI/FEDER, UE) and from Universitat Rovira i Virgili (URV) (Spain) through grant PFR 2021PFR-URV-144. In addition, the authors want to thank Professor Joan Rosell LLompart (URV, Spain) for fruitful discussions.

Conflicts of Interest: The authors declare no conflict of interest. The funders had no role in the design of the study; in the collection, analyses, or interpretation of data; in the writing of the manuscript; or in the decision to publish the results.

References

1. Sundar, S.; Kundu, J.; Kundu, S.C. Biopolymeric Nanoparticles. *Sci. Technol. Adv. Mater.* **2010**, *11*, 14104. [[CrossRef](#)]
2. Thirugnanasambandan, T. *Bio-Nanocomposites in Biomedical Application BT—Polymer Based Bio-Nanocomposites: Properties, Durability and Applications*; Muthukumar, C., Thiagamani, S.M.K., Krishnasamy, S., Nagarajan, R., Siengchin, S., Eds.; Springer: Singapore, 2022; pp. 275–291. ISBN 978-981-16-8578-1.
3. Almería, B.; Deng, W.; Fahmy, T.M.; Gomez, A. Controlling the Morphology of Electrospray-Generated PLGA Microparticles for Drug Delivery. *J. Colloid Interface Sci.* **2010**, *343*, 125–133. [[CrossRef](#)]
4. Nath, S.D.; Son, S.; Sadiasa, A.; Min, Y.K.; Lee, B.T. Preparation and Characterization of PLGA Microspheres by the Electrospraying Method for Delivering Simvastatin for Bone Regeneration. *Int. J. Pharm.* **2013**, *443*, 87–94. [[CrossRef](#)]
5. Beneš, M.; Pekárek, T.; Beránek, J.; Havlíček, J.; Krejčík, L.; Šimek, M.; Tkadlecová, M.; Doležal, P. Methods for the Preparation of Amorphous Solid Dispersions—A Comparative Study. *J. Drug Deliv. Sci. Technol.* **2017**, *38*, 125–134. [[CrossRef](#)]
6. Patterson, J.E.; James, M.B.; Forster, A.H.; Lancaster, R.W.; Butler, J.M.; Rades, T. Preparation of Glass Solutions of Three Poorly Water Soluble Drugs by Spray Drying, Melt Extrusion and Ball Milling. *Int. J. Pharm.* **2007**, *336*, 22–34. [[CrossRef](#)] [[PubMed](#)]
7. Tran, P.; Pyo, Y.C.; Kim, D.H.; Lee, S.E.; Kim, J.K.; Park, J.S. Overview of the Manufacturing Methods of Solid Dispersion Technology for Improving the Solubility of Poorly Water-Soluble Drugs and Application to Anticancer Drugs. *Pharmaceutics* **2019**, *11*, 132. [[CrossRef](#)] [[PubMed](#)]
8. Boel, E.; Koekoek, R.; Dedroog, S.; Babkin, I.; Vetrano, M.R.; Clasen, C.; Van Den Mooter, G. Unraveling Particle Formation: From Single Droplet Drying to Spray Drying and Electrospraying. *Pharmaceutics* **2020**, *12*, 625. [[CrossRef](#)] [[PubMed](#)]
9. Vehring, R.; Snyder, H.; Lechuga-Ballesteros, D. Spray Drying. *Dry. Technol. Biotechnol. Pharm. Appl.* **2020**, *7*, 179–216.
10. Wang, S.; Langrish, T. A Review of Process Simulations and the Use of Additives in Spray Drying. *Food Res. Int.* **2009**, *42*, 13–25. [[CrossRef](#)]
11. Bohr, A.; Kristensen, J.; Dyas, M.; Edirisinghe, M.; Stride, E. Release Profile and Characteristics of Electrosprayed Particles for Oral Delivery of a Practically Insoluble Drug. *J. R. Soc. Interface* **2012**, *9*, 2437–2449. [[CrossRef](#)]
12. Littringer, E.M.; Zellnitz, S.; Hammernik, K.; Adamer, V.; Friedl, H.; Urbanetz, N.A. Spray Drying of Aqueous Salbutamol Sulfate Solutions Using the Nano Spray Dryer B-90—The Impact of Process Parameters on Particle Size. *Dry. Technol.* **2013**, *31*, 1346–1353. [[CrossRef](#)]
13. Bhujbal, S.V.; Mitra, B.; Jain, U.; Gong, Y.; Agrawal, A.; Karki, S.; Taylor, L.S.; Kumar, S.; Zhou, Q. Pharmaceutical Amorphous Solid Dispersion: A Review of Manufacturing Strategies. *Acta Pharm. Sin. B* **2021**, *11*, 2505–2536. [[CrossRef](#)] [[PubMed](#)]
14. Tamber, H.; Johansen, P.; Merkle, H.P.; Gander, B. Formulation Aspects of Biodegradable Polymeric Microspheres for Antigen Delivery. *Adv. Drug Deliv. Rev.* **2005**, *57*, 357–376. [[CrossRef](#)] [[PubMed](#)]
15. Varde, N.K.; Pack, D.W. Microspheres for Controlled Release Drug Delivery. *Expert Opin. Biol. Ther.* **2004**, *4*, 35–51. [[CrossRef](#)]
16. Sosnik, A.; Seremeta, K.P. Advantages and Challenges of the Spray-Drying Technology for the Production of Pure Drug Particles and Drug-Loaded Polymeric Carriers. *Adv. Colloid Interface Sci.* **2015**, *223*, 40–54. [[CrossRef](#)]
17. Bock, N.; Dargaville, T.R.; Woodruff, M.A. Electrospraying of Polymers with Therapeutic Molecules: State of the Art. *Prog. Polym. Sci.* **2012**, *37*, 1510–1551. [[CrossRef](#)]
18. Bodnár, E.; Grifoll, J.; Rosell-Llompart, J. Polymer Solution Electrospraying: A Tool for Engineering Particles and Films with Controlled Morphology. *J. Aerosol Sci.* **2018**, *125*, 93–118. [[CrossRef](#)]
19. Almería, B.; Gomez, A. Electrospray Synthesis of Monodisperse Polymer Particles in a Broad (60 nm–2 µm) Diameter Range: Guiding Principles and Formulation Recipes. *J. Colloid Interface Sci.* **2014**, *417*, 121–130. [[CrossRef](#)]
20. Hogan, C.J.; Yun, K.M.; Chen, D.R.; Lenggono, I.W.; Biswas, P.; Okuyama, K. Controlled Size Polymer Particle Production via Electrohydrodynamic Atomization. *Colloids Surf. A Physicochem. Eng. Asp.* **2007**, *311*, 67–76. [[CrossRef](#)]
21. Rosell-Llompart, J.; Grifoll, J.; Loscertales, I.G. Electrosprays in the Cone-Jet Mode: From Taylor Cone Formation to Spray Development. *J. Aerosol Sci.* **2018**, *125*, 2–31. [[CrossRef](#)]
22. Bohr, A.; Wan, F.; Kristensen, J.; Dyas, M.; Stride, E.; Baldursdóttir, S.; Edirisinghe, M.; Yang, M. Pharmaceutical Microparticle Engineering with Electrospraying: The Role of Mixed Solvent Systems in Particle Formation and Characteristics. *J. Mater. Sci. Mater. Med.* **2015**, *26*, 61. [[CrossRef](#)]
23. Nguyen, D.N.; Clasen, C.; Van den Mooter, G. Pharmaceutical Applications of Electrospraying. *J. Pharm. Sci.* **2016**, *105*, 2601–2620. [[CrossRef](#)]
24. Moreira, A.; Lawson, D.; Onyekuru, L.; Dziemidowicz, K.; Angkawitwong, U.; Costa, P.F.; Radacsi, N.; Williams, G.R. Protein Encapsulation by Electrospinning and Electrospraying. *J. Control. Release* **2021**, *329*, 1172–1197. [[CrossRef](#)]
25. Danhier, F.; Ansorena, E.; Silva, J.M.; Coco, R.; Le Breton, A.; Préat, V. PLGA-Based Nanoparticles: An Overview of Biomedical Applications. *J. Control. Release* **2012**, *161*, 505–522. [[CrossRef](#)]
26. Ahmad, Z.; Mehta, P.; Zaman, A.; Smith, A.; Rasekh, M.; Haj-Ahmad, R.; Arshad, S.; Merwe, S.; Chang, M.-W.; Ahmad, Z. Broad Scale and Structure Fabrication of Healthcare Materials for Drug and Emerging Therapies via Electrohydrodynamic Techniques. *Adv. Ther.* **2018**, *2*, 1800024. [[CrossRef](#)]
27. Yaghoobi, N.; Majidi, R.F.; Faramarzi, M.A.; Baharifar, H.; Amani, A. Preparation, Optimization and Activity Evaluation of PLGA/Streptokinase Nanoparticles Using Electrospray. *Adv. Pharm. Bull.* **2017**, *7*, 131–139. [[CrossRef](#)]

28. Jahangiri, A.; Davaran, S.; Fayyazi, B.; Tanhaei, A.; Payab, S.; Adibkia, K. Application of Electro spraying as a One-Step Method for the Fabrication of Triamcinolone Acetonide-PLGA Nanofibers and Nanobeads. *Colloids Surf. B Biointerfaces* **2014**, *123*, 219–224. [[CrossRef](#)]
29. Lee, P.W.; Pokorski, J.K. Poly(Lactic-Co-Glycolic Acid) Devices: Production and Applications for Sustained Protein Delivery. *Wiley Interdiscip. Rev. Nanomed. Nanobiotechnol.* **2018**, *10*, e1516. [[CrossRef](#)]
30. Liu, K.; Sun, Z.; Nie, M.; Wu, Y. Electro spraying in Carbon Dioxide-Expanded Antisolvent. *J. Supercrit. Fluids* **2015**, *103*, 122–129. [[CrossRef](#)]
31. Rezvanpour, A.; Attia, A.B.E.; Wang, C.H. Enhancement of Particle Collection Efficiency in Electrohydrodynamic Atomization Process for Pharmaceutical Particle Fabrication. *Ind. Eng. Chem. Res.* **2010**, *49*, 12620–12631. [[CrossRef](#)]
32. Shen, S.-J.; Chou, Y.-C.; Hsu, S.-C.; Lin, Y.-T.; Lu, C.-J.; Liu, S.-J. Fabrication of Ropivacaine/Dexamethasone-Eluting Poly(D, L-Lactide-Co-Glycolide) Microparticles via Electro spraying Technique for Postoperational Pain Control. *Polymers* **2022**, *14*, 702. [[CrossRef](#)] [[PubMed](#)]
33. Tanaka, M.; Ochi, A.; Sasai, A.; Tsujimoto, H.; Kobara, H.; Yamamoto, H.; Wakisaka, A. Biodegradable PLGA Microsphere Formation Mechanisms in Electro sprayed Liquid Droplets. *KONA Powder Part. J.* **2022**, 2022018. [[CrossRef](#)]
34. Xu, J.; Li, K.; Liu, M.; Gu, X.; Li, P.; Fan, Y. Studies on Preparation and Formation Mechanism of Poly(Lactide-Co-Glycolide) Microrods via One-Step Electro spray and an Application for Drug Delivery System. *Eur. Polym. J.* **2021**, *148*, 110372. [[CrossRef](#)]
35. Baldino, L.; Cardea, S.; Reverchon, E. Supercritical Assisted Electro spray: An Improved Micronization Process. *Polymers* **2019**, *11*, 244. [[CrossRef](#)]
36. Baldino, L.; Cardea, S.; Reverchon, E. A Supercritical CO₂ Assisted Electrohydrodynamic Process Used to Produce Microparticles and Microfibers of a Model Polymer. *J. CO₂ Util.* **2019**, *33*, 532–540. [[CrossRef](#)]
37. Campardelli, R.; Baldino, L.; Reverchon, E. Supercritical Fluids Applications in Nanomedicine. *J. Supercrit. Fluids* **2015**, *101*, 193–214. [[CrossRef](#)]
38. Guastaferrero, M.; Baldino, L.; Cardea, S.; Reverchon, E. Supercritical Assisted Electro spray/Spinning to Produce PVP+quercetin Microparticles and Microfibers. *J. Taiwan Inst. Chem. Eng.* **2020**, *117*, 278–286. [[CrossRef](#)]
39. Guastaferrero, M.; Cardea, S.; Baldino, L.; Reverchon, E. Cellulose Acetate Nanocarrier Production by Supercritical Assisted Electro spray. *Chem. Eng. Trans.* **2021**, *87*, 391–396. [[CrossRef](#)]
40. Husain, O.; Lau, W.; Edirisinghe, M.; Parhizkar, M. Investigating the Particle to Fibre Transition Threshold during Electrohydrodynamic Atomization of a Polymer Solution. *Mater. Sci. Eng. C* **2016**, *65*, 240–250. [[CrossRef](#)]
41. Carrasco-Munoz, A.; Barbero-Colmenar, E.; Bodnár, E.; Grifoll, J.; Rosell-Llompart, J. Monodisperse Droplets and Particles by Efficient Neutralization of Electro sprays. *J. Aerosol Sci.* **2022**, *160*, 105909. [[CrossRef](#)]
42. Hartman, R.P.A.; Brunner, D.J.; Camelot, D.M.A.; Marijnissen, J.C.M.; Scarlett, B. Jet Break-up in Electrohydrodynamic Atomization in the Cone-Jet Mode. *J. Aerosol Sci.* **2000**, *31*, 65–95. [[CrossRef](#)]
43. Enayati, M.; Chang, M.W.; Bragman, F.; Edirisinghe, M.; Stride, E. Electrohydrodynamic Preparation of Particles, Capsules and Bubbles for Biomedical Engineering Applications. *Colloids Surf. A Physicochem. Eng. Asp.* **2011**, *382*, 154–164. [[CrossRef](#)]